Magnetic Exchange in Transition Metal Complexes. 12.[1] Calculation of Cluster Exchange Coupling Constants with the Xα-Scattered Wave Method

A. P. Ginsberg

Contribution from Bell Laboratories, Murray Hill, New Jersey 07974.
Received June 28, 1979

Abstract: A first principles calculation of cluster exchange coupling constants (i.e., J_{ab} in the total spin Hamiltonian $H_{ex} = -2\sum_{\text{atom pairs},a,b} J_{ab}\mathbf{S}_a\cdot\mathbf{S}_b$) is attempted within the framework of the standard SCF-Xα-SW method. The results for the triply Cl bridged dimer $Mo_2Cl_9^{3-}$ in the salts $Cs_3Mo_2Cl_9$ (d(Mo-Mo) = 2.655 Å) and $K_3Mo_2Cl_9$ (d(Mo-Mo) = 2.53 Å) are J_{ab}(calcd) = −355 and −1268 cm^{-1}, respectively. The corresponding experimental values are −421 and −556 cm^{-1}. From the calculated electronic structure of $Mo_2Cl_9^{3-}$, the exchange coupling mechanism is seen to be purely direct metal-metal interaction with no superexchange. The presence of Mo-Mo bonding which resides in a predominantly Mo-bridging Cl orbital, and is quite distinct from the coupling of the magnetic electrons, is also revealed by the calculations. It is concluded that, while there is much room for improvement, the standard SCF-Xα-SW method is useful in studying exchange coupling in clusters.

Introduction

Exchange coupling between metal atoms in single-ion orbital singlet ground states has been extensively investigated in cluster complexes.[2] It has been found that the exchange split cluster energy levels are generally given by the total spin form of the spin-coupling Hamiltonian

$$H_{ex} = -2\sum_{\substack{\text{atom}\\ \text{pairs}\\ a,b}} J_{ab}\mathbf{S}_a\cdot\mathbf{S}_b \qquad (1)$$

where J_{ab} is the exchange coupling constant for the intracluster interaction between metal atoms at sites a and b with total spin operators $\mathbf{S}_a$ and $\mathbf{S}_b$. Comparison of experimental susceptibility vs. temperature measurements with the susceptibility equation derived from eq 1 enables the J_{ab} to be evaluated. Exchange coupling constants for a large number of cluster complexes have been determined in this way.

In contrast to the profuse experimental measurements of cluster exchange constants, attempts at theoretical calculation of these quantities have been very limited in number. The problem is difficult because it requires the calculation of small energy differences (<1000 cm^{-1}) in large many-electron systems, and because it is necessary to take account of electron correlation.

All of the calculations of J_{ab} that have so far been reported are semiempirical in nature. Most of these are based on Anderson's theory[3,4] and the configuration interaction method of Keffer and Oguchi[5] and Huang and Orbach,[6,7] and make heavy use of experimental data and free-atom wave functions for estimating the many integrals involved. More recently,[8] a calculation based on Heitler-London wave functions including admixture of ionic states led to an expression for dimer exchange constants in terms of one-electron orbital splittings and overlaps. With orbital energies obtained from extended Hückel calculations, it proved possible to understand qualitatively the changes in J_{ab} with structure and substituents for a variety of Cu^{2+} dimers; however, calculated values of J_{ab} were not reported. A new model for estimating dimer exchange constants was recently proposed by Kahn and Briat.[9-11] These authors used Heitler-London wave functions *without* admixed ionic states to obtain a relation between J_{ab} and one-electron orbital splittings and overlaps. In the case of $[Cr_2O_{10}]^{14-}$ and $[Cr_2Cl_9]^{3-}$, Kahn and Briat obtained the correct numerical magnitude for J_{ab} using orbital energies calculated with extended Hückel theory.

With the advent of the Xα-SW method[12,13] it has become possible to attempt completely nonempirical, self-consistent-field calculations of cluster exchange constants. That such calculations might give useful results is suggested by the following considerations: (a) Inherent in the Xα method is an approximate description of electron correlation.[14-16] (b) Spin-unrestricted calculations can be carried out.[17] (c) The transition-state method[18] may be used to obtain the energy separation between spin states of a system in terms of orbital energy differences. These energy differences may then be related to the exchange coupling constant.[19]

Analysis of the problem reveals that the relation between J_{ab} and spin state splittings calculated by the Xα method is quite approximate. This approximation is the best that can be achieved if the calculations are to be carried out entirely within the framework of the SCF-Xα-SW method as implemented in the standard programs. To determine if reasonable values for cluster exchange coupling constants can be obtained in this way, it is necessary to carry out calculations for appropriate systems. In this paper I report results for the complex $[Mo_2Cl_9]^{3-}$. This system was chosen because it exhibits significantly different Mo-Mo distances in its potassium and cesium salts, and the difference is reflected in the observed exchange coupling constants. Thus, for $Cs_3Mo_2Cl_9$[20-22] d(Mo-Mo) = 2.655 Å and J_{ab} (obsd) = −421 cm^{-1}, while for $K_3Mo_2Cl_9$[21,23] d(Mo-Mo) = 2.53 Å and J_{ab} (obsd) = −556 cm^{-1}. By calculating J_{ab} for $Mo_2Cl_9^{3-}$ with structural parameters for both the cesium and potassium salts, a test is obtained of the ability of the theory to account for the effects of small structural changes on exchange coupling. The calculated values of J_{ab} are of the correct sign and order of magnitude, and qualitatively reproduce the difference between the Cs and K salts. The calculations also provide an illuminating description of the exchange coupling in $Mo_2Cl_9^{3-}$, and reveal the existence of weak metal-metal bonding quite distinct from the coupling of the magnetic electrons. While these are notable accomplishments for a first principles theory and indicate that the proposed method is useful, its inherently approximate nature must be borne in mind. Further tests of the method on other clusters are highly desirable.

Theory

The total spin Hamiltonian eq 1 for a dimer leads to a simple relation between J_{ab} and spin state total energy differences:

$$J_{ab} = \frac{1}{S_2'(S_2'+1) - S_1'(S_1'+1)}[E(S_1') - E(S_2')] \qquad (2)$$

0002-7863/80/1502-0111$01.00/0

where S_1' and S_2' are allowed values of the total dimer spin ($S_2' > S_1'$): $S_1', S_2' = (S_a + S_b), (S_a + S_b - 1), \cdots |S_a - S_b|$. It is the objective of this work to test the possibility of evaluating J_{ab} by using the standard SCF-Xα-SW programs to calculate the spin state total energy difference in eq 2. In order to understand the limitations of such calculations it is necessary to review part of the derivation of eq 1.

It can be shown that, for the case of orbital singlet magnetic ions at sites a and b, the general expression for the exchange operator reduces to[24]

$$\mathbf{H}_{ex} = \sum_{ij} - 2\mathcal{J}_{ij}\mathbf{s}_a\cdot\mathbf{s}_b \tag{3}$$

in which i and j run over all magnetic (i.e., singly occupied) orbitals Φ_{ai} and Φ_{bj} and where $\mathbf{s}_a$ and $\mathbf{s}_b$ are spin half operators at sites a and b, respectively. $\mathcal{J}_{ij}$ is the exchange coupling constant for the interaction between magnetic orbitals Φ_{ai} and Φ_{bj}, which are localized on the centers a and b, respectively. In order to transform eq 3 to the total spin form, it is necessary to invoke the Hund's rule restriction which constrains the magnetic electrons on the single ions to have parallel spins. If the single-ion total spin is S, then within the $|S, M|$ manifold

$$\mathbf{s}_a = \frac{1}{2S}\mathbf{S}_a \tag{4}$$

$$\mathbf{s}_b = \frac{1}{2S}\mathbf{S}_b$$

$$\mathbf{s}_a\cdot\mathbf{s}_b = \frac{1}{4S^2}\mathbf{S}_a\cdot\mathbf{S}_b$$

Making the definition

$$J_{ij} = \left(\frac{1}{4S^2}\right)\mathcal{J}_{ij} \tag{5}$$

we can write

$$\sum_{ij} - 2\mathcal{J}_{ij}\mathbf{s}_a\cdot\mathbf{s}_b = \sum_{ij} - 2J_{ij}\mathbf{S}_a\cdot\mathbf{S}_b = - 2J_{ab}\mathbf{S}_a\cdot\mathbf{S}_b \tag{6}$$

We may now examine the relationship between the dimer spin states of eq 2 and the dimer spin states which can be represented within the framework of the standard Xα method. First of all note that in the spin polarized Xα description the lowest energy electron configuration with all magnetic electrons in spin up molecular orbitals corresponds uniquely to the S' = maximum state, while the lowest energy configuration with ½ of the magnetic electrons in spin up and ½ in spin down MOs corresponds uniquely to the $S' = 0$ state. On the other hand, for an S' value intermediate between 0 and the maximum, more than one electron configuration can always be written. Hence it is only for $S' = 0$ and S' = maximum that we can correlate a spin state of eq 2 with an Xα configuration state. Making this correlation we write

$$J_{ab} \approx \frac{1}{S'_{max}(S'_{max}+1)}[\langle E(S'=0)\rangle_{X\alpha} - \langle E(S'=S'_{max})\rangle_{X\alpha}] \tag{7}$$

Now recall the fact, emphasized by Slater[14] and noted by others,[15,16] that the Xα method includes the effect of electronic correlation to a sufficient degree of approximation that it correctly describes the limiting behavior of a diatomic molecule as the interatomic distance is increased. For a *weakly* coupled dimer we may therefore expect that the Xα configuration state with S' = maximum corresponds with a state in which the single ions have their magnetic electrons entirely in localized spin up orbitals. The Xα configuration state with $S' = 0$, on the other hand, corresponds to a state in which the single ions each have their magnetic electrons equally distributed among localized spin-up and spin-down orbitals (effective atomic spin $S = 0$). We see then that, while $\langle E(S' = \text{maximum})\rangle_{X\alpha}$ should be a good approximation to the energy of the S' = maximum state of eq 2, $\langle E(S'=0)\rangle_{X\alpha}$ is a poor approximation for the energy of the $S' = 0$ state. Equation 7 is therefore a drastic approximation, but it is the best that can be done within the framework of the standard Xα method.

In order to implement eq 7 it is necessary to decide upon a method for calculating the Xα total energy difference. There are three possible approaches: (1) separate calculation of $\langle E(S'=0)\rangle_{X\alpha}$ and $\langle E(S'=S'_{max})\rangle_{X\alpha}$ and taking the difference; (2) the generalized transition state method;[26] (3) incremental single electron transition state calculations.[26] Method (1) is unsatisfactory for a system such as $[Mo_2Cl_9]^{3-}$ because of the difficulty of accurately determining by direct calculation small differences between numerically very large total energies. Methods (2) and (3) overcome this difficulty by relating the total energy difference to a sum of Xα orbital energies.

For a multielectron excitation of a system with M levels, the generalized transition state approximation is[26]

$$\langle E_F\rangle_{X\alpha} - \langle E_I\rangle_{X\alpha} = \sum_{i=1}^{M}\Delta n_i\epsilon_{0i} + \frac{\Delta\alpha}{\alpha_0}E_{0x} \tag{8}$$

where the ϵ_{0i} are the Xα orbital energies in the transition state, defined as the state with occupation numbers

$$n_{0i} = \frac{1}{2}(n_{Ii} + n_{Fi}) \tag{9}$$

exchange correlation parameter

$$\alpha_0 = \frac{1}{2}(\alpha_I + \alpha_F) \tag{10}$$

and Xα exchange energy E_{0x}. Δn_i is the change in occupation number in the ith orbital on going from the initial to the final state:

$$\Delta n_i = n_{Fi} - n_{Ii} \tag{11}$$

while $\Delta\alpha$ is the change in the exchange correlation parameter:

$$\Delta\alpha = \alpha_F - \alpha_I \tag{12}$$

In the present application, the change from the initial to the final state consists in moving the $\frac{1}{2}S'_{max}$ highest energy spin-down electrons into the same number of empty lowest spin-up orbitals. Since the metal atoms are only weakly interacting the overall electronic structure in the initial and final states must be similar. It will therefore be assumed that $\Delta\alpha = 0$ so that eq 8 reduces to

$$\langle E_F\rangle_{X\alpha} - \langle E_I\rangle_{X\alpha} = \sum_{i=1}^{M}\Delta n_i\epsilon_{0i} \tag{13}$$

The generalized transition state form of eq 7 may now be written as

$$J_{ab} \approx \frac{1}{S'_{max}(S'_{max}+1)}\sum_{i=1}^{M}\Delta n_i\epsilon_{0i} \tag{14}$$

where

$$\Delta n_i = n_i(S'=0) - n_i(S'=\text{max}) \tag{15}$$

The incremental method for calculating the Xα total energy difference in eq 7 consists of breaking the multielectron excitation up into a sum of single-electron excitations and calculating the energy of each of these with the Slater transition state method. Recent atomic Xα calculations[26b] have shown the incremental method to be, in general, a more accurate procedure for calculating the Xα total energy change of a multielectron excitation than is the generalized transition state method. However, when the initial and final orbitals for the excitation are similar, as they are in the calculation of J_{ab}, the

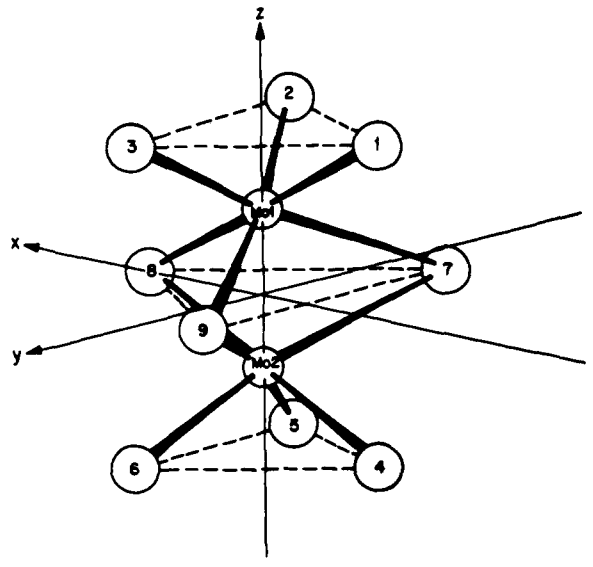

Figure 1. Coordinate axes, geometry, and atom labeling scheme for $Mo_2Cl_9^{3-}$ (D_{3h}).

Table I. $Mo_2Cl_9^{3-}$ Bond Lengths (Å) and Angles (deg) in the Cs^+ and K^+ Salts

	$Cs_3Mo_2Cl_9$[a]	$K_3Mo_2Cl_9$[b]
d Mo-Mo	2.655	2.53
d Mo-Cl(term.)	2.384	2.39
d Mo-Cl (bridge)	2.487	2.51
$\angle Cl_t$-Mo-Cl_t	91.0	90.5
$\angle Cl_{br}$-Mo-Cl_{br}	94.2	97
$\angle$Mo-Cl_{br}-Mo	64.5	60.5

[a] From ref 22. [b] From ref 23.

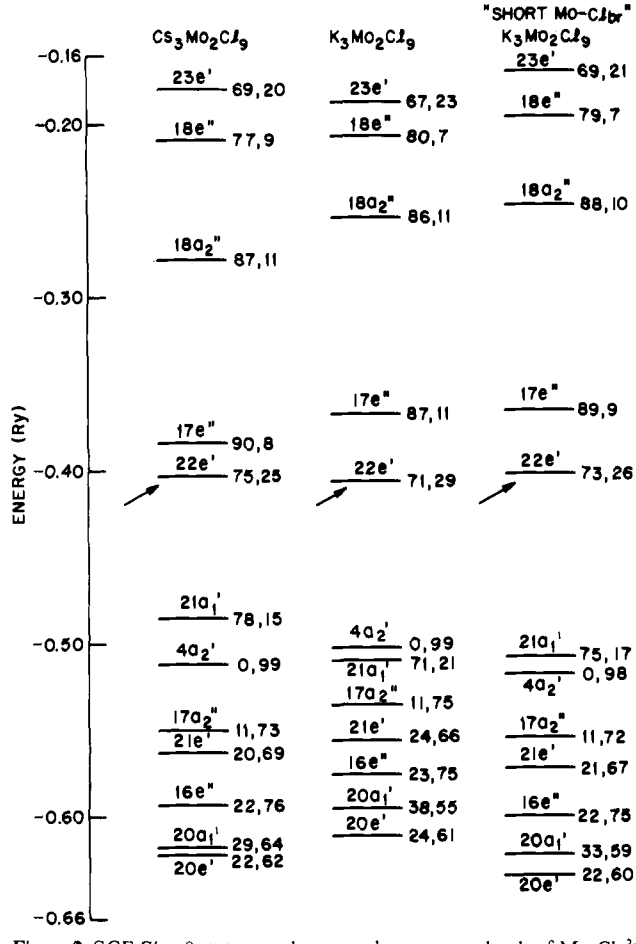

Figure 2. SCF $S' = 0$ state one-electron valence energy levels of $Mo_2Cl_9^{3-}$ with predominantly Mo 4d or Cl_{br} 3p character. The arrows point to the highest occupied levels. The numbers to the right of each level are the relative (%) amounts of charge within the 2Mo and $3Cl_{br}$ spheres, respectively; they differ from the values in Table III in being normalized so that % 2Mo + % $3Cl_{br}$ + % $6Cl_t$ = 100. The energy levels from the $K_3Mo_2Cl_9$ and the "short Mo-Cl_{br}" $K_3Mo_2Cl_9$ calculations were uniformly scaled, by addition of 0.034 Ry in the first case and 0.014 Ry in the second, in order to bring the Cl_t 3s nonbonding levels into coincidence with the $Cs_3Mo_2Cl_9$ values.

two methods should be comparable in accuracy. In the present work on $Mo_2Cl_9^{3-}$ both methods were used and it was found that both give very similar results for J_{ab}. This is an important finding since it indicates that the generalized transition state method, which requires considerably less computation than the incremental method, may be used for implementing eq 7.

Procedure for Calculations on $[Mo_2Cl_9]^{3-}$

SCF-Xα-SW calculations were carried out in double precision on a Honeywell 6000 computer, using current versions of the programs written originally by K. H. Johnson and F. C. Smith.

Figure 1 shows the coordinate axes and atom numbering scheme for $Mo_2Cl_9^{3-}$ (point group symmetry D_{3h}). Table I summarizes the important bond lengths and angles as found in the cesium and potassium salts. Coordinates in atomic units (1 bohr = 0.529 17 Å) were derived from the values in Table I and are summarized in Table II. A third set of coordinates in Table II corresponds to the Mo-Mo distance in $K_3Mo_2Cl_9$, but with the Mo-Cl (bridge) distance shortened by 0.06 Å; these values were used in a calculation to evaluate the contribution of Cl bridge orbitals to the exchange coupling. Table II also contains the sphere radii used in the calculations. Overlapping atomic sphere radii were obtained by scaling the atomic number radii[27] so as to optimize the ground-state virial ratio at self-consistency. The outer sphere surrounding the molecule was centered on the origin and assigned a radius which made it tangent to the terminal Cl atomic spheres when the radii were scaled to give terminal Cl and Mo spheres which touched. This gave an overlapping outer sphere for the actual atomic sphere radii.[27] A Watson sphere[28] with radius equal to the mean Cs^+ or K^+ distance from the dimer origin,[29] and bearing a +3 charge, was used to simulate the electrostatic interaction of the dimer with its surrounding crystal lattice. α exchange-correlation parameters for Mo and Cl were from Schwarz's tables[30,31] (α_{HF}(Mo) = 0.703 41, α_{HF}(Cl) = 0.723 25). In the extramolecular and intersphere regions α was taken as an average of α(Mo) and α(Cl) weighted by the number of valence electrons in the atoms (α(OUT) = α(INT) = 0.716 22).

The highest order spherical harmonics used to expand the wave functions were $l = 4$ in the extramolecular region, $l = 2$ in the Mo spheres, and $l = 1$ in the Cl spheres. SCF calculations of the $S' = 0$ ground state were spin restricted and converged to ±0.0005 Ry or better for each level. Core levels were not frozen at any point. All transition-state calculations were spin polarized and were iterated until the levels of interest had convered to ±0.0005 Ry or better. In determining J_{ab} by the generalized transition state method, using eq 14, a value was calculated for each of five to ten iterations preceding the final iteration. Plots of the J_{ab} values against ΔJ_{ab}, the change from one iteration to the next, were linear, and least-squares extrapolation to $\Delta J_{ab} = 0$ gave the final result. A similar procedure was used to calculate J_{ab} by the incremental transition state method, except that in this case it was the single electron

Table II. Atomic Coordinates and Sphere Radii for $Mo_2Cl_9^{3-}$ (bohrs)

salt	region	x	y	z	R^a
$Cs_3Mo_2Cl_9$	Mo(1)	0	0	2.508 65	2.573 68
	Mo(2)	0	0	−2.508 65	2.573 68
	Cl(1)	−3.7120	0	5.0617	2.505 23
	Cl(2)	1.8560	−3.2147	5.0617	2.505 23
	Cl(3)	1.8560	3.2147	5.0617	2.505 23
	Cl(4)	−3.7120	0	−5.0617	2.505 23
	Cl(5)	1.8560	−3.2147	−5.0617	2.505 23
	Cl(6)	1.8560	3.2147	−5.0617	2.505 23
	Cl(7)	−1.9872	−3.4418	0	2.429 55
	Cl(8)	3.9743	0	0	2.429 55
	Cl(9)	−1.9872	3.4418	0	2.429 55
	OUT	0	0	0	8.499 16
	Watson	0	0	0	7.638 4
$K_3Mo_2Cl_9$	Mo(1)	0	0	2.3905	2.553 12
	Mo(2)	0	0	−2.3905	2.553 12
	Cl(1)	−3.7038	0	4.9753	2.488 55
	Cl(2)	1.8519	−3.2076	4.9753	2.488 55
	Cl(3)	1.8519	3.2076	4.9753	2.488 55
	Cl(4)	−3.7038	0	−4.9753	2.488 55
	Cl(5)	1.8519	−3.2076	−4.9753	2.488 55
	Cl(6)	1.8519	3.2076	−4.9753	2.488 55
	Cl(7)	−2.0642	−3.5388	0	2.423 17
	Cl(8)	4.0968	0	0	2.423 17
	Cl(9)	−2.0642	3.5388	0	2.423 17
	OUT	0	0	0	8.431 86
	Watson	0	0	0	7.325 6
"$K_3Mo_2Cl_9$" with Mo-Cl_{br} shortened to 2.45 Å[b]	Mo(1)	0	0	2.3905	2.568 28
	Mo(2)	0	0	−2.3905	2.568 28
	Cl(1)	−3.7120	0	4.9436	2.524 83
	Cl(2)	1.8560	−3.2147	4.9436	2.524 83
	Cl(3)	1.8560	3.2147	4.9436	2.524 83
	Cl(4)	−3.7120	0	−4.9436	2.524 83
	Cl(5)	1.8560	−3.2147	−4.9436	2.524 83
	Cl(6)	1.8560	3.2147	−4.9436	2.524 83
	Cl(7)	−1.9872	−3.4418	0	2.430 77
	Cl(8)	3.9743	0	0	2.430 77
	Cl(9)	−1.9872	3.4418	0	2.430 77
	OUT	0	0	0	8.415 49
	Watson	0	0	0	7.325 6

[a] $Cs_3Mo_2Cl_9$: R = 0.8724 (atomic no. radii). $K_3Mo_2Cl_9$: R = 0.8659 (atomic no. radii). "$K_3Mo_2Cl_9$" with short Mo-Cl_{br}: R = 0.879 89 (atomic no. radii). [b] Same x and y coordinates as $Cs_3Mo_2Cl_9$, but z coordinates changed by axial compression to d Mo-Mo = 2.53 Å.

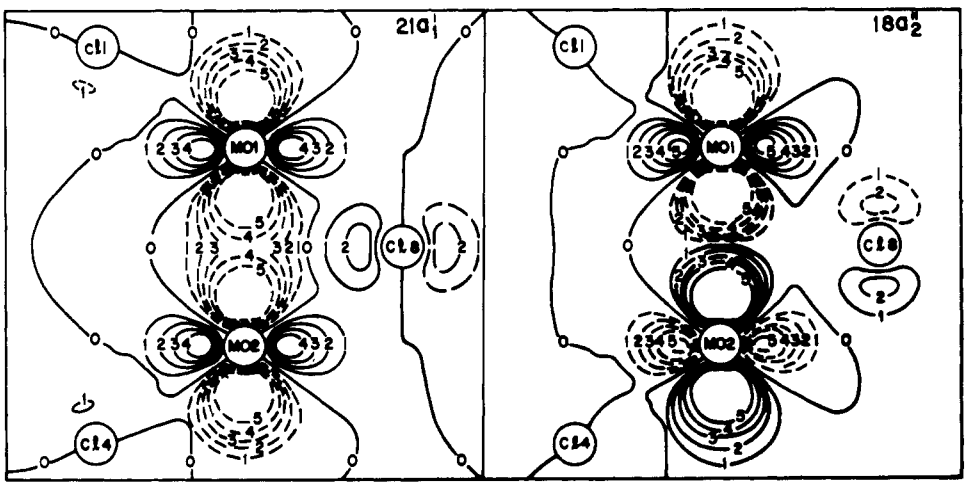

Figure 3. Wave function contour maps of the $Mo_2Cl_9^{3-}$ S' = 0 state $21a_1'$ and $18a_2''$ orbitals in the xz plane (Cs salt calculation). Solid and broken lines denote contours of opposite sign having magnitudes indicated by the numerical labels: 0, 1, 2, 3, 4 = 0, 0.04, 0.06, 0.08, 0.10, 0.13 (electrons/bohr^3)$^{1/2}$, respectively.

excitation energies, into which the total multielectron excitation was decomposed, which were extrapolated to zero change from one iteration to the next.

Results

The $Mo_2Cl_9^{3-}$ S' = 0 state valence energy levels, charge distributions, and orbital descriptions from the $Cs_3Mo_2Cl_9$

Table III. $Mo_2Cl_9^{3-}$ $S' = 0$ State Valence Energy Levels, Charge Distributions, and Orbital Descriptions from the $Cs_3Mo_2Cl_9$ Calculation

level[a]	energy, Ry	charge distribution, %[b] 2Mo	$6Cl_t$	$3Cl_{br}$	INT	OUT	major Mo spherical harmonics[c]	description
24e′	−0.085	3[d]	2[d]	7[d]	53[d]	35[d]		
$22a_1'$	−0.124	1	3	3	59	35		
23e′	−0.180	54	8	16	17	5	$d_{xz,yz}$, $d_{x^2-y^2,xy}$	Mo-Cl_{br} antibonding
18e″	−0.209	68	12	8	10	2	$d_{xz,yz}$, $d_{x^2-y^2,xy}$	Mo-Cl antibonding
$18a_2''$	−0.278	78	2	10	10	0	d_{z^2}	σ-Mo-Mo antibonding; Mo, Cl nonbonding
17e″	−0.384	81	2	7	10	0	$d_{x^2-y^2,xy}$, $d_{xz,yz}$	π-Mo-Mo antibonding; Mo, Cl nonbonding
22e′	−0.403	64	0	21	14	0	$d_{x^2-y^2,xy}$, $d_{xz,yz}$	π-Mo-Mo bonding; Mo, Cl nonbonding
$21a_1'$	−0.485	69	7	13	11	0	d_{z^2}	σ-Mo-Mo bonding; Mo, Cl nonbonding
$4a_2'$	−0.512	0	1	78	20	0		Cl_{br} 3p nonbonding
$17a_2''$	−0.550	9	13	61	16	1		Cl_{br} 3p nonbonding
21e′	−0.563	16	9	56	18	0	$d_{x^2-y^2,xy}$	Mo-Cl_{br} bonding
16e″	−0.593	17	2	60	20	0	$d_{x^2-y^2,xy}$	Mo-Cl_{br} bonding
$20a_1'$	−0.617	24	6	53	16	0	d_{z^2}, p_z, s	Mo-Cl_{br} and Mo-Mo bonding
20e′	−0.622	18	13	51	17	0	$d_{xz,yz}$, $p_{x,y}$	Mo-Cl_{br} bonding
$2a_1''$	−0.744	0	87	0	12	1		Cl_t 3p nonbonding
$3a_2'$	−0.748	0	86	1	14	0		Cl_t 3p nonbonding
15e″	−0.759	1	84	0	14	1		Cl_t 3p nonbonding
19e′	−0.771	4	76	3	16	0		Cl_t 3p nonbonding
14e″	−0.781	2	21	57	18	1		Cl_{br} and Cl_t 3p nonbonding
18e′	−0.782	12	66	6	16	0	$d_{yz,yz}$	Mo-Cl_t bonding
$19a_1'$	−0.793	9	77	2	13	2		Cl_t 3p nonbonding
$16a_2''$	−0.803	5	74	3	16	2		Cl_t 3p nonbonding
13e″	−0.824	17	75	0	5	2	$d_{xz,yz}$, $d_{x^2-y^2,xy}$ $p_{x,y}$	Mo-Cl_t bonding
$15a_2'$	−0.830	8	77	2	11	2	s, p_z	Mo-Cl_t bonding
$18a_1'$	−0.835	9	75	2	13	1	s	Mo-Cl_t bonding
17e′	−0.837	21	68	4	5	2	$d_{xz,yz}$, $d_{x^2-y^2,xy}$	Mo-Cl_t bonding
16e′	−1.392	3	0	89	8	0		Cl_{br} 3s nonbonding
$17a_1'$	−1.394	2	1	88	9	0		Cl_{br} 3s nonbonding
15e′	−1.652	2	93	0	4	1		Cl_t 3s nonbonding
12e″	−1.652	2	93	0	4	1		Cl_t 3s nonbonding
$14a_2''$	−1.661	2	92	0	6	1		Cl_t 3s nonbonding
$16a_1'$	−1.663	2	91	0	6	1		Cl_t 3s nonbonding

[a] The highest occupied level is 22e′. [b] Percentage of the total population of a given level located within the combined molybdenum (2Mo), combined terminal chlorine ($6Cl_t$), combined bridging chlorine ($3Cl_{br}$), intersphere (INT), and extramolecular (OUT) regions. The *total* charge distribution in electrons is 81.80 in 2Mo, 97.77 in $6Cl_t$, 50.05 in 3 Cl_{br}, 9.76 in INT, and 0.61 in OUT. [c] Spherical-harmonic basis functions contributing more than 10% of the Mo charge, in order of decreasing importance. [d] From the $K_3Mo_2Cl_9$ calculation.

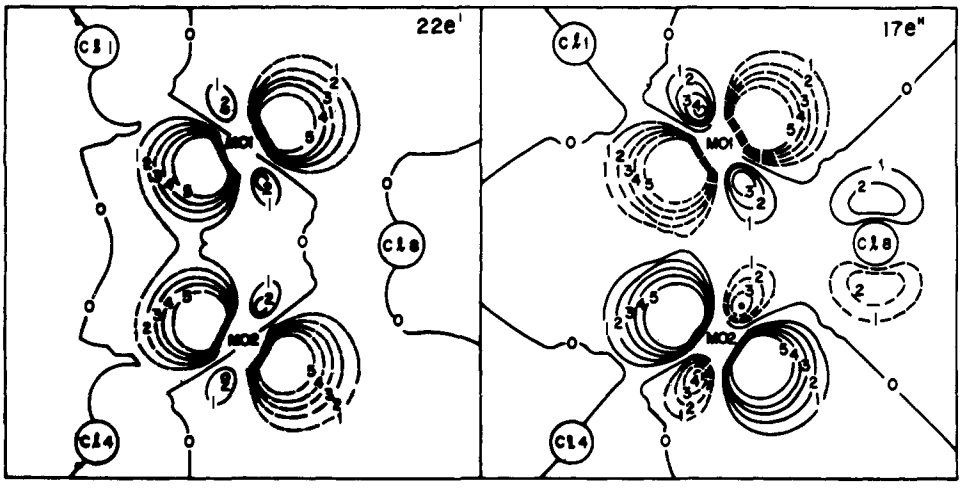

Figure 4. Wave function contour maps of the $Mo_2Cl_9^{3-}$ $S' = 0$ state 22e′ and 17e″ orbitals in the *xz* plane (Cs salt calculation). Contour magnitudes and sign convention as in Figure 3.

calculation are summarized in Table III. Details of the $K_3Mo_2Cl_9$ $S' = 0$ state calculations are not tabulated, but levels with predominantly Mo 4d or Cl_{br} 3p character from all three calculations are plotted in Figure 2. Figures 3 and 4 are contour maps of the Mo-Mo bonding and antibonding MOs with predominantly (64-81%) Mo character. Figure 5 shows contours for the $20a_1'$ Mo-Cl_{br}, Mo-Mo bonding orbital. These maps were each generated from the numerical values

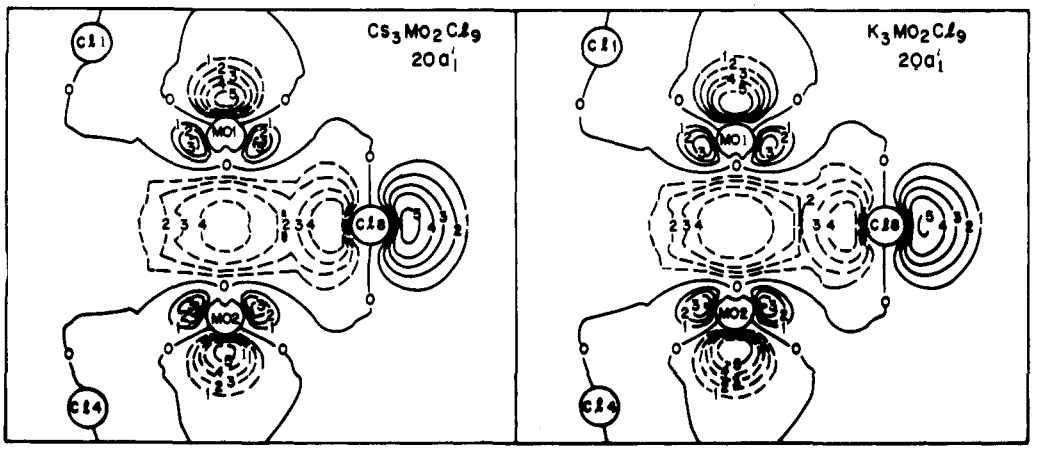

Figure 5. Wave function contour maps of the $Mo_2Cl_9^{3-}$ $S' = 0$ state $20a_1'$ orbital in the xz plane for $Cs_3Mo_2Cl_9$ and $K_3Mo_2Cl_9$. Contour magnitudes and sign convention as in Figure 3.

Table IV. Calculated and Observed Exchange Coupling Constants for $Mo_2Cl_9^{3-}$

system	calcd J_{ab}, cm^{-1} generalized tr state method	calcd J_{ab}, cm^{-1} incremental tr state method	obsd J_{ab}, cm^{-1}
$Cs_3Mo_2Cl_9$	−355		−421[a]
$K_3Mo_2Cl_9$	−1268	−124[a]	−556[b]
"short Mo-Cl_{br} $K_3Mo_2Cl_9$"	−1266		

[a] Reference 20. [b] Reference 21.

of the wave functions at 6561 grid points within a 16 × 16 $bohr^2$ area centered on the origin. Table IV is a summary of the calculated exchange coupling constants. The final virial ratios for the three $S' = 0$ calculations were as follows: $Cs_3Mo_2Cl_9$, 0.999 995 7; $K_3Mo_2Cl_9$, 0.999 990 3; "short Mo-Cl_{br} $K_3Mo_2Cl_9$," 1.000 010.

Discussion

Table III provides a picture of the $S' = 0$ state electronic structure of $Mo_2Cl_9^{3-}$ in $Cs_3Mo_2Cl_9$; essentially the same overall picture is obtained from the $K_3Mo_2Cl_9$ calculations. The valence energy levels of $Mo_2Cl_9^{3-}$ can be separated more or less clearly into eight groups. In order of increasing energy these are (1) six nearly pure Cl 3s nonbonding levels in the range −1.66 to −1.39 Ry; (2) four levels in the range −0.84 to −0.82 Ry which are the main Mo-terminal Cl bonding orbitals; (3) a group of eight levels in the range −0.80 to −0.74 Ry, of which six are predominantly terminal Cl 3p nonbonding in character while one has significant Mo-Cl_t bonding character and one is mostly nonbonding Cl_{br} 3p; (4) four levels between −0.62 and −0.56 Ry which are the major Mo-bridging Cl bonding orbitals (one of these, $20a_1'$, also has significant σ-Mo-Mo bonding character); (5) a pair of predominantly Cl_{br} 3p nonbonding levels between −0.55 and −0.51 Ry; (6) four levels ($21a_1'$, 22e′, 17e″, and $18a_2''$) with 64-81% Mo 4d character in the range −0.48 to −0.28 Ry. These are the MOs which mediate the weak interaction between the single-ion magnetic electrons. As may be seen from the contour maps in Figure 3, level $21a_1$ corresponds to a σ-Mo-Mo bonding orbital formed by interaction of the essentially $4d_{z^2}$ single-ion magnetic orbitals. Level $18a_2''$ is its antibonding counterpart and is unoccupied in the $S' = 0$ state. Similarly Figure 4 shows that level 22e′ (the HOMO) corresponds to a very weakly bonding π-Mo-Mo orbital, one component of which is formed by interaction of hybrid d_{xz}, $d_{x^2-y^2}$ single-ion magnetic orbitals. Level 17e″ is its antibonding counterpart and is unoccupied in the $S' = 0$ state. (7) Above the Mo-Mo antibonding orbitals are a pair of Mo-Cl antibonding orbitals (18e″ and 23e′) with 54-68% Mo character. (8) Finally, at still higher energies levels $22a_1'$ and 24e′ have only 7-12% of their charge localized within the atomic spheres and are diffuse Rydberg-state orbitals.

The increased Mo-Mo interaction in $K_3Mo_2Cl_9$, brought about by the shorter Mo-Mo distance, is reflected in the energy level diagram of Figure 2. The major change from $Cs_3Mo_2Cl_9$ to $K_3Mo_2Cl_9$ is the increased bonding-antibonding splitting between levels $21a_1'$ and $18a_2''$ and between 22e′ and 17e″. In fact, in the $K_3Mo_2Cl_9$ diagram $21a_1'$ falls below the Cl_{br} 3p nonbonding $4a_2'$ level. Another difference between the Cs and K salts which is evident in Figure 2 is a slight weakening of the Mo-Cl_{br} bonding interaction. This is shown by the increased energy of the Mo-Cl_{br} bonding orbitals in $K_3Mo_2Cl_9$ while the Mo-Cl_{br} antibonding orbital (23e′) is lowered in energy. Associated with this is an increased Mo sphere and decreased Cl_{br} sphere charge in the bridge bonding orbitals of the potassium salt. Figure 5 shows clearly the greater Mo-Cl_{br} overlap in the $20a_1'$ bridge bonding orbital of the cesium as compared to the potassium salt. Also to be noted, for later discussion, is the somewhat increased Cl_{br} sphere charge, at the expense of the Mo sphere, in the Mo-Mo bonding orbitals of the potassium salt. Thus in orbital 22e′ there is a 4% increase in the Cl_{br} sphere charge and a 4% decrease in the Mo sphere while in the $21a_1'$ level there is a 6% charge transfer from the Mo to the Cl_{br} sphere.

Figure 5, in addition to showing the Mo-Cl_{br} overlap in orbital $20a_1'$, reveals that this orbital has considerable Mo-Mo bonding character. In fact orbital $20a_1'$ has the largest direct Mo-Mo overlap of any orbital in the cluster. Since this interaction is not canceled by an equivalent antibonding interaction in any of the occupied orbitals, we may conclude that there is present in $Mo_2Cl_9^{3-}$ significant net Mo-Mo bonding quite distinct from the weak coupling of the magnetic orbitals. Similar weak direct Fe-Fe bonding has recently been shown to be present in $Fe_2S_2(SH)_4^{2-}$, where it is concentrated in a mainly Fe-(bridging S) orbital.[32]

In order to calculate J_{ab} via eq 7 it is necessary to determine the Xα total energy difference between the $S' = 0$ state and the $S' = 3$ state with electron configuration $\ldots(22e\uparrow)^2(21a_1'\uparrow)^1(17e''\uparrow)^2(18a_2''\uparrow)^1$. Even in the case of $K_3Mo_2Cl_9$, where level $21a_1'$ lies below level $4a_2'$ in the $S' = 0$ state, the latter configuration gives the lowest energy $S' = 3$ state, being 0.0646 Ry below the $\ldots(22e'\uparrow)^2(4a_2'\uparrow)^1(17e''\uparrow)^2(18a_2''\uparrow)^1$ configuration. The transition-state configuration for calculating $\langle E(S' = 0)\rangle_{X\alpha} - \langle E(S' = 3)\rangle_{X\alpha}$ with eq 14 is $\ldots(21a_1'\uparrow)^1(21a_1'\downarrow)^{0.5}(22e'\uparrow)^2(17e''\uparrow)^1(22e'\downarrow)^1(18a_2''\uparrow)^{0.5}$. In the incremental transition state calculation, the total energy

difference was calculated in three parts using single electron transition states which corresponded to successively flipping spins $22e'\downarrow \rightarrow 17e''\uparrow$, $22e'\downarrow \rightarrow 17e''\uparrow$, and $21a_1'\downarrow \rightarrow 18a_2''\uparrow$. As may be seen in Table IV, the two methods of calculation gave close agreement in the $K_3Mo_2Cl_9$ case; other calculations were therefore carried out using only the generalized transition state method. The calculated value of J_{ab} for $Cs_3Mo_2Cl_9$ is in quite good agreement with experiment, being only 16% too small in magnitude. However, J_{ab} (calcd) for $K_3Mo_2Cl_9$ is 128% too large in magnitude. The calculated increase in $|J_{ab}|$ from the cesium to the potassium salt is thus much larger than observed (913 vs. 135 cm^{-1}).[33]

A question which often arises in discussions of exchange coupling is: What is the relative importance of superexchange and of direct metal-metal interaction in the coupling mechanism? According to Anderson's theory superexchange occurs when metal atom magnetic orbitals are delocalized by overlap with bridging ligand atom orbitals so that the interaction between spins on different metal atoms is enhanced. The question of superexchange vs. direct metal-metal interaction in any given case is then simply a question of the extent to which overlap of single-ion magnetic orbitals is determined by ligand atom contributions. In the case of $Mo_2Cl_9^{3-}$ we have seen that the structural change from the cesium to the potassium salt causes some redistribution of charge between the Mo and Cl_{br} spheres in the Mo-Cl_{br} and in the Mo-Mo bonding orbitals. To the extent that superexchange is significant in $Mo_2Cl_9^{3-}$, the charge redistribution may be contributing to the change in J_{ab}. The question may be addressed in two ways. First of all we see from Figures 2-4 that, although the Mo-Mo bonding orbitals place significant amounts of charge within the Cl_{br} sphere, this charge is nonbonding and does not make any significant contribution to the Mo-Mo overlap in either the 22e' or $21a_1'$ orbitals. Secondly, by carrying out a calculation for an $Mo_2Cl_9^{3-}$ system with d(Mo-Mo) the same as in $K_3Mo_2Cl_9$ but with d(Mo-Cl_{br}) contracted to 2.45 Å, it is found (Figure 2) that the charge distribution in the Mo-Cl_{br} and in the Mo-Mo bonding orbitals is nearly the same as for the $Cs_3Mo_2Cl_9$ case, but the calculated J_{ab} is changed only slightly from the $K_3Mo_2Cl_9$ value. The Xα analysis therefore leads to the conclusion that the exchange coupling in $Mo_2Cl_9^{3-}$ is a case of pure metal-metal interaction with no superexchange.

The results in this paper indicate that the standard SCF-Xα-SW method can be useful in the study of cluster exchange coupling. There appear to be two avenues open for improving the calculations. The first would require an improved Xα description of the $S' = 0$ state. A theory which may accomplish this is the Xα-VB method being developed by Noodleman and Norman.[34] It will be of great interest to see what success this theory has in calculating exchange coupling constants. Another approach, which is now being investigated, is to circumvent the problem of the poor description of the $S' = 0$ state by calculating J_{ab} entirely within the S' = maximum state. This can be accomplished by using a relation of the type recently derived by Hay et al.[8] or Kahn and Briat.[10]

References and Notes

(1) Part 11: A. P. Ginsberg, M. E. Lines, K. D. Karlin, S. J. Lippard, and F. J. DiSalvo, *J. Am. Chem. Soc.*, **98**, 6958 (1976).
(2) For reviews see (a) R. L. Martin in "New Pathways in Inorganic Chemistry", E. A. V. Ebsworth, A. G. Maddock, and A. G. Sharpe, Eds., Cambridge University Press, New York, 1968. Chapter 9; (b) A. P. Ginsberg, *Inorg. Chim. Acta Rev.*, **5**, 45 (1971); (c) D. J. Hodgson, *Prog. Inorg. Chem.*, **19**, 173 (1975).
(3) P. W. Anderson, *Phys. Rev.*, **115**, 2 (1959).
(4) P. W. Anderson, *Solid State Phys.*, **14**, 99-214 (1963).
(5) F. Keffer and T. Oguchi, *Phys. Rev.*, **115**, 1428 (1959).
(6) N. L. Huang and R. Orbach, *Phys. Rev.*, **154**, 487 (1967); N. L. Huang, *ibid.*, **157**, 378 (1967).
(7) C. G. Barraclough and R. W. Brookes, *J. Chem. Soc., Faraday Trans. 2*, **70**, 1364 (1974).
(8) P. J. Hay, J. C. Thibeault, and R. Hoffman, *J. Am. Chem. Soc.*, **97**, 4884 (1975).
(9) O. Kahn and B. Briat, *J. Chem. Soc., Faraday Trans. 2*, **72**, 268 (1976).
(10) O. Kahn and B. Briat, *J. Chem. Soc., Faraday Trans. 2*, **72**, 1441 (1976).
(11) O. Kahn, B. Briat, and J. Galy, *J. Chem. Soc., Dalton Trans.*, 1453 (1977).
(12) K. H. Johnson, *Annu. Rev. Phys. Chem.*, **26**, 39 (1975).
(13) J. C. Slater, "The Self-Consistent Field for Molecules and Solids: Quantum Theory of Molecules and Solids", Vol. 4, McGraw-Hill, New York, 1974.
(14) Reference 13, pp 83-86.
(15) R. P. Messmer and D. R. Salahub, *J. Chem. Phys.*, **65**, 779 (1976).
(16) F. A. Cotton and G. C. Stanley, *Inorg. Chem.*, **16**, 2668 (1977).
(17) Reference 13, Chapter 3.
(18) Reference 13, pp 7-8 and 51-55.
(19) The calculation of exchange constants in terms of the splittings between cluster spin states, as carried out in this work, differs from the method proposed by Slater for calculating the exchange constant of a ferromagnetic crystal by the Xα-SW method (ref 13, pp 191-194).
(20) I. E. Grey and P. W. Smith, *Aust. J. Chem.*, **22**, 121 (1969).
(21) I. E. Grey and P. W. Smith, *Aust. J. Chem.*, **24**, 73 (1971).
(22) R. Saillant, R. B. Jackson, W. E. Streib, K. Folting, and R. A. D. Wentworth, *Inorg. Chem.*, **10**, 1453 (1971).
(23) I. E. Grey and P. W. Smith, *Aust. J. Chem.*, **22**, 1627 (1969).
(24) The general theory is in ref 3 and 4. Reference 25 gives the most general form of the exchange operator. For a concise derivation of eq 3 from the general expression see the Appendix in ref 1.
(25) F. Hartmann-Boutron, *J. Phys. (Paris)*, **29**, 212 (1968).
(26) (a) A. R. Williams, R. A. de Groot, and C. B. Sommers, *J. Chem. Phys.*, **63**, 628 (1975); (b) A. P. Ginsberg, to be published.
(27) J. G. Norman, Jr., *Mol. Phys.*, **31**, 1191 (1976).
(28) R. E. Watson, *Phys. Rev.*, **111**, 1108 (1958).
(29) $Cs_3Mo_2Cl_9$ has two Cs^+ at 3.9392 and one at 4.2476 Å from the dimer origin. In $K_3Mo_2Cl_9$ the corresponding distances are 3.7622 Å for two K^+ and 4.1050 Å for one.
(30) K. Schwarz, *Phys. Rev. B*, **5**, 2466 (1972).
(31) K. Schwarz, *Theor. Chim. Acta*, **34**, 225 (1974).
(32) J. G. Norman, B. J. Kalbacher, and S. C. Jackels *J. Chem. Soc., Chem. Commun.*, 1027 (1978).
(33) The sensitivity of the J_{ab} calculation to the choice of atomic sphere radii was investigated. It was found that a 2% decrease in the sphere radius scale factor results in a ca. 100-cm^{-1} decrease in the magnitude of J and a ca. 75-ppm increase in the virial ratio. The effect of the Watson sphere radius on J_{ab} (calcd) was also investigated. Choosing the Watson sphere radius as described in the text or taking it to have the same radius as the outer sphere both give essentially the same result for J_{ab} (calcd).
(34) L. Noodleman and J. G. Norman Jr., *J. Chem. Phys.*, **70**, 4903 (1979).